Aquatic Toxicology 286 (2025) 107430

Contents lists available at ScienceDirect

Aquatic Toxicology

journal homepage: www.elsevier.com/locate/aqtox

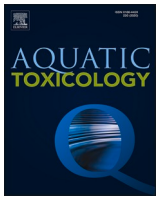

Comparative assessment of uptake and effects of TiO_2 and CeO_2 nanoparticles in Algae using advanced single-entity analytical techniques

Mariam Bakir [a], Isabel Abad-Alvaro [b], Francisco Laborda [b], Vera I. Slaveykova [a,*]

[a] Environmental Biogeochemistry and Ecotoxicology, Department F.A. Forel for Environmental and Aquatic Sciences, Faculty of Sciences, University of Geneva, 66 Blvd Carl-Vogt, CH 1211, Geneva, Switzerland
[b] Group of Analytical Spectroscopy and Sensors (GEAS), Institute of Environmental Sciences (IUCA), University of Zaragoza, Pedro Cerbuna, 12 50009, Zaragoza, Spain

ARTICLE INFO

Keywords:
Ecotoxicity
Nanomaterials
Hormesis
Raphidocellis subcapitata
Flow cytometry
Oxidative stress
SP- ICP-MS
SC-ICP-MS

ABSTRACT

Despite significant progress in understanding the toxicity of engineered nanoparticles (NPs) in aquatic environments, key gaps remain in our understanding of their uptake and effects on algae. Specifically, it is unclear whether NPs must be internalized and cross biological membranes to induce toxicity, or if surface interactions alone are sufficient. This study aimed to explore the relationship between uptake and effects of TiO_2-NPs and CeO_2-NPs on the green alga Raphidocelis subcapitata using advanced single-entity analytical techniques. Flow cytometry was used to distinguish algal cells from NP aggregates and determine growth rates, while single-cell inductively coupled plasma mass spectrometry (SC-ICP-MS) quantified adsorbed and internalized metals, operationally discriminated by washing cycles with EDTA. Single-particle ICP-MS (SP-ICP-MS) characterized NP size distribution and dissolution. Results showed greater toxicity for CeO_2-NPs (72h-EC_{50} of 13.6 ± 0.57 mg L^{-1}) compared to TiO_2-NPs (72h-EC_{50} of 28.3 ± 1.16 mg L^{-1}), with hormesis observed for TiO_2-NPs between 11 and 20 mg L^{-1}. CeO_2-NPs. induced a significantly higher level of ROS production, showing a 71.8 % increase compared to the unexposed control, whereas TiO_2-NPs induced only a 39.46 % increase at highest tested concentration of 50 mg L^{-1}. SC-ICP-MS revealed both adsorption and internalization of NPs, with Ti accumulation exceeding Ce, despite that CeO_2-NPs induced stronger growth inhibition and oxidative stress. Hetero-aggregation between NPs and algae, along with changes in cell granularity, was observed at higher NP concentrations. These findings offer insights into TiO_2-NPs and CeO_2-NPs interactions with microalgae and highlight the importance of advanced analytical techniques in assessing nanoparticle behavior in aquatic ecosystems.

1. Introduction

The use of engineered nanoparticles (NPs) has grown rapidly due to their unique physicochemical properties, with applications in various industries such as medicine, agriculture, cosmetics, and electronics (Altammar, 2023). However, this increasing use raises environmental concerns, as NPs can be released throughout their life cycle and have the potential to adversely affect aquatic organisms, including phytoplankton (Bundschuh et al., 2018; Lead et al., 2018; Nguyen et al., 2020; Yu et al., 2025; Zeng, Y.L. et al., 2024).

The present study focuses on two widely used NPs of significant interest due to their diverse applications: TiO_2-NPs (Dar et al., 2020) and CeO_2-NPs (Pansambal et al., 2022). TiO_2-NPs are commonly used in products like paints, toothpaste, sunscreens, and photocatalysis (Musial et al., 2020), while CeO_2-NPs are applied in photocatalysis and biomedical applications, including antibacterial and antioxidant treatments (Pansambal et al., 2022). Both types of NPs have been studied for their toxicity in phytoplankton species, such as *Raphidocelis subcapitata, Chlamydomonas reinhardtii*, and *Chlorella vulgaris*, with concentration that causes a 50 % effect on algal growth (EC_{50}) values typically in the mg L^{-1} range (Lee et al., 2022; Liu, 2021; Rivero Arze et al., 2020; Xie et al., 2021; Yu et al., 2025; Zeng, H. et al., 2024). Toxicity also varies by species – CeO_2-NPs were more toxic to cyanobacterium *Anabaena* CPB4337 than to green alga *R. subcapitata* (Rodea-Palomares et al., 2011). ROS generation is frequently cited as a key toxicity mechanism for both NP types (Dobesova et al., 2023; Liu et al., 2024, 2022; Sivakumar et al., 2025; Wu et al., 2022; Xie et al., 2021), though some studies report minimal ROS-related effects, particularly under prolonged exposure (Angel et al., 2015; Siciliano et al., 2024). Other mechanisms, such as physical entrapment and hetero-aggregation, may also

* Corresponding author.
E-mail address: vera.slaveykova@unige.ch (V.I. Slaveykova).

https://doi.org/10.1016/j.aquatox.2025.107430
Received 7 April 2025; Received in revised form 22 May 2025; Accepted 27 May 2025
Available online 29 May 2025

contribute to toxicity by limiting nutrient and light availability (Joonas et al., 2019; Mahaye and Musee, 2023; Wang et al., 2024). As no ion release has been observed, toxicity is attributed to the particles themselves (Hund-Rinke et al., 2018). However, it remains unclear whether the NPs have to be internalized and cross biological membranes to induce toxicity or if only the surface interaction between the NPs and the cells can produce toxicity in cells.

Despite the advancements in bioaccumulation research in algae (Zheng and Nowack, 2022), the current literature regarding NP uptake in phytoplankton is rather limited and presents divergent findings. For example, internalization of CeO_2-NP has been reported in the cyanobacteria *Nostoc muscorum* and *Anabaena laxa* (Hamed et al., 2024), as well as within vesicles of the green alga *C. reinhardtii* (Pulido-Reyes et al., 2019; Taylor et al., 2016). However, in some species, such as cyanobacterium *Microcystis aeruginosa* (Wu et al., 2022) and green alga *C. reinhardtii* (Kosak Nee Rohder et al., 2018), no internalization was detected, though strong membrane adsorption was reported. These discrepancies highlight a species-specific and context-dependent behavior of NP uptake, which remains poorly understood. Furthermore, while surface adsorption is often mentioned as a key process, there is a lack of clarity on the relative contribution of internalization versus adsorption to overall toxicity and bioaccumulation. The fate of internalized NPs, including possible transformation, compartmentalization, or excretion, is also largely unexplored. These knowledge gaps suggest that methodological limitations (e.g., reliance on microscopy or indirect measurements) may contribute to inconsistent interpretations.

The use of advanced single-entity analytical techniques such as single-cell inductively coupled plasma mass spectrometry (SC-ICP-MS) offers a way toward resolving these inconsistencies. Unlike conventional methods, SC-ICP-MS allows for quantitative, high-resolution detection of metal-based NPs in individual cells without pretreatment. By measuring specific isotopes, SC-ICP-MS provides high sensitivity and accuracy, making it a valuable tool in ecotoxicology. It has been used to detect CeO_2-NPs (Mackevica et al., 2023), Ag-NPs in *R. subcapitata* (Bakir et al., 2024) and *C. vulgaris* (Lum and Leung, 2019) and Au-NPs in *Cyptomonas ovate* (Merrifield et al., 2018). However, its application to comparative studies across different NP types and algal species is still limited.

This study leverages advanced single-particle and single-cell analytical techniques to comprehensively assess the uptake and toxicity of TiO_2-NPs and CeO_2-NPs in the green alga *R. subcapitata*. Flow cytometry (FCM) was used to differentiate algal cells from NP aggregates, allowing for precise cell count determination, for assessment of NP-cell interactions and effects on individual cells in the algal populations. SC-ICP-MS quantified the levels of adsorbed and intracellular metals per cell, while single-particle inductively coupled plasma mass spectrometry (SP-ICP-MS) was used to characterize NP size distribution and dissolution. The unique combination of these single-entity analytical techniques (SP-ICP-MS, SC-ICP-MS and FCM) enables novel and complementary insights across elemental content, particle size, cell treats and fluorescence. Despite targeting different parameters, all three techniques share the key advantage of resolving heterogeneity at the level of individual cells or NPs (Haddad et al., 2023). Few studies integrate these complementary single-entity techniques to explore NP uptake and biological effects at such resolution. Based on existing literature, we hypothesize that biological responses in algae are linked to NP adsorption and potential penetration of biological membranes (Mahana et al., 2021; von Moos et al., 2014; Yu et al., 2025). Green alga *R. subcapitata* was chosen as a representative phytoplankton species, given its role as a primary producer in aquatic systems and a key link in the food chain. This comprehensive approach offers valuable insights into NP-algae interactions.

2. Materials and methods

2.1. Reagents and chemicals

The nanopowders, TiO_2 (NM-102-JRCNM10202) and CeO_2 (NM-212-JRCNM02102), were acquired from the Nanomaterials Repository at the European Commission Joint Research Centre (JRC) (Ispra, Italy). Details of their composition, size, zeta potential or water solubility, among others, are described in (Rasmussen et al., 2014) for TiO_2-NPs and in (Singh et al., 2014) for CeO_2-NPs, and summarized in Table S1 in Supporting Information (SI). The stock suspensions were prepared by adding 15 mg of TiO_2-NPs or CeO_2-NPs to 5 mL of ultrapure water (Milli-Q Advantage, Molsheim, France) in glass vials to get a final concentration of 3000 mg L^{-1}. Then, the suspensions were sonicated in an ultrasonic bath at 40 mHz for 15 min (Branson 5510 MT Ultrasonic Cleaner, Branson Ultrasonics Corporation, Danbury, USA).

For the analysis by ICP-MS, ionic Ti with a concentration of 998 ± 2 mg L^{-1} (Fluka Analytical, Buchs, Switzerland) was used. AuNPs of 50.2 nm and 0.5 mg L^{-1} (Nanocomposix, San Diego, CA, USA) were used to obtain the transport efficiency by SP-ICP-MS and SC-ICP-MS.

2.2. Characterization of tio_2-nps and ceo_2-nps suspensions

The size distribution in the suspension of the NPs was performed using SP-ICP-MS (Agilent 7700 ICP-MS, Morges, Switzerland). The acquisition parameters utilized for the analysis are detailed in Table S2. Prior to analysis, the instrument performance was optimized using a solution containing 1 μg L^{-1} of Ce, Co, Li, Mg, Tl, and Y in 2 % HNO_3. Additionally, the sample flow rate was determined gravimetrically, and the transport efficiency (TE) was measured to ensure an accurate analysis of the samples. TE was calculated using the frequency method (Pace et al., 2011), employing a suspension of 50 nm AuNPs at a concentration of 4.36×10^7 particles L^{-1}. For TiO_2-NP analysis, a calibration curve ranging from 0 to 5 μg L^{-1} of ionic Ti in 1 % HNO_3 was used. In the case of CeO_2-NPs, the calibration curve, also ranging from 0 to 5 μg L^{-1}, was based on the same particles, given the distinct behavior of nanoparticles compared to their ionic forms (Sanchez-Garcia et al., 2016).

The NPs suspensions were also analyzed by dynamic light scattering (DLS) (PN3700, Zetasizer Nano) to obtain the hydrodynamic size and aggregation state, as well as the zeta potential.

2.3. Algal cultivation

The choice of alga *R. subcapitata* was based on the recommendation of the Organization for Economic Co-operation and Development (OECD) for conducting ecotoxicity tests (OECD, 2011). This alga (SKULBERG 1959/1 strain) was exposed to nanoparticles in a Tris acetate phosphate (TAP) medium, whose composition is in Table S3, starting with an initial concentration of 3×10^5 cells mL^{-1}. Cultivation was carried out in an incubator (Infors HT Multitron, Infors, Basel, Switzerland) at a controlled temperature of 20.1 ± 0.2 °C, with shaking at 100 rpm, and under a light: dark cycle of 16:8 hours. At the middle of the exponential growth phase, the algae have been isolated and resuspended in the TAP exposure medium, whose composition is in Table S4, enriched with TiO_2-NPs or CeO_2-NPs.

The concentrations in the growth inhibition test vary in a large range: from 0.3 to 100 mg L^{-1} for TiO_2-NPs and from 0.1 to 100 mg L^{-1} for CeO_2-NPs. Although these concentrations are much higher than those found in freshwater environments (e.g. <100 ng L^{-1} CeO_2-NPs and <10 μg L^{-1} TiO_2-NPs) (Azimzada et al., 2021), they encompass ranges that are both ecotoxicologically relevant (Kahru and Ivask, 2013) and significant for regulatory assessment. According to the EU CLP Regulation (EC No 1272/2008) and OECD guidelines, pollutants that do not exhibit significant toxicity at or below 100 mg L^{-1} in acute aquatic tests are generally considered not acutely hazardous. All the experiments were conducted in triplicate. Unexposed algae were used as a negative

control.

2.4. Assessment of the effect of TiO_2-NPS and CeO_2-NPS on algae

The effect of NPs on cell number, chlorophyll autofluorescence and granularity was assessed using flow cytometer (BD Accuri C6 Plus flow cytometer, BD, New Jersey, USA), equipped with a CSampler (BD Biosciences, San Jose, CA). The 488-nm argon excitation laser and fluorescence detection channels with band pass emission filters at 530 ± 15 nm (FL1), 585 ± 20 nm (FL2) and a long pass emission filter for > 670 nm (FL3) were used. A threshold of 20,000 events was set within the algae gate in the chlorophyll autofluorescence cytogram to ensure good data accuracy. Data acquisition and analysis were performed with the BD Accuri C6 Software 264.15. The algae gate used to ensure the distinction between algae and NPs aggregates of comparable size is detailed in Fig. S1. With the cell density obtained by FCM, the growth rates were calculated with Eq. (1), where $\mu_{i\text{-}j}$ is the average growth rate from time i to time j and X_j and X_j are the cell densities at time i and j.

$$\mu_{i-j} = \frac{\ln X_j - \ln X_i}{t_j - t_i} \ (day^{-1}) \quad (1)$$

The growth rate inhibition of cells exposed to varying concentrations of TiO_2-NPs and CeO_2-NPs, relative to unexposed controls (growth rate of 0.301 ± 0.071 d^{-1}), was calculated over a 72 h exposure period. The fitting for TiO_2-NPs followed the equation proposed by (Deng et al., 2012), while the fitting for CeO_2-NPs was performed using the Hill equation.

The effect of TiO_2-NPs and CeO_2-NPs on cellular *granularity* was assessed using Side scatter signal (SSC). Changes in *chlorophyll fluorescence* of the algal cells were determined via FCM using FL3 channel. To assess possible *membrane damage* induced by the NPs at the end of the 72 h exposure, the cells were analyzed by FCM after staining with propidium iodide (PI) as previously detailed (Cheloni et al., 2014; von Moos et al., 2015). After a 72-h exposure, PI (Sigma-Aldrich, Buchs, Switzerland) was added to the algae at a final concentration of 7 μmol L^{-1}, then incubated for 30 min in the dark and measured using FCM on channel FL-2. Cells heated at 90 °C for 30 min were used as positive control, whereas unexposed cells served as a negative control. The impact of NPs on cellular ROS levels was evaluated using a Synergy H1 microplate reader (Biotek, Santa Clara, USA). To this end, cells were incubated with CellROX® Green reagent (Thermo Fisher Scientific, Waltham, MA, USA) at a final concentration of 10 μM for 1 h in the dark at 37 °C. As a positive control, cells were exposed to 20 % hydrogen peroxide for 30 min. Following exposure and reagent addition, fluorescence was measured with an excitation wavelength of 488 nm and an emission wavelength of 530 nm.

2.5. Uptake of the TiO_2-NPS and CeO_2-NPS by R. subcapitata

To study NPs uptake by algae, including both adsorbed and intracellular fractions, SC-ICP-MS (Perkin Elmer NexION 2000B, Perkin Elmer, Toronto, Canada) with an Asperon™ linear pass spray chamber (Perkin Elmer, Toronto, Canada) and a flow-focusing nebulizer (Ingeniatrics, Sevilla, Spain) was employed. After 72 h of exposure, the suspensions of algae were centrifuged and the pellets were collected. The cells were also washed with 0.02 mol L^{-1} of ethylenediaminetetraacetic acid (EDTA) five times to remove the surface-adsorbed (EDTA-extractable) NPs (Kosak Nee Rohder et al., 2018; Thiagarajan et al., 2019). Both "washed", and "unwashed" cells were analyzed to differentiate between adsorbed and intracellular metal concentrations. Before analysis by SC-ICP-MS, the collected pellets were resuspended in 50 mL of ultrapure water, followed by appropriate dilutions. Instrumental optimization was performed using a 1 μg L^{-1} multielement solution containing Be, Ce, Fe, In, Li, Mg, Pb and U. The acquisition parameters were optimized with a solution of 5 μg L^{-1} of TiO_2 in 1 % of HNO_3 and 1 μg L^{-1} of CeO_2-NPs. To avoid the interference of Ca and P in the analysis of TiO_2-NPs, ammonia was used as a reaction gas in the reaction cell. For Ti, the ratio *m/z* 131 was measured since no interferences were observed with this adduct ($^{48}Ti(NH)(NH_3)_4$) (Suárez-Oubiña et al., 2022). The potential interferences with Ca were evaluated using suspensions containing 5 μg L^{-1} of Ti and increasing concentrations of Ca, ranging from 10 μg L^{-1} to 10 mg L^{-1}. It was observed that minor interferences occurred starting at 1 mg L^{-1} of Ca. For CeO_2, no interferences were detected, and thus, no reaction gas was required. Due to the differing behavior of ionic Ce and CeO_2-NPs, reflected in the distinct slopes of their calibration curves (5.55×10^4 counts (μg L^{-1})$^{-1}$ for ionic Ce and 3.02×10^4 counts (μg L^{-1})$^{-1}$ for CeO_2-NPs), a calibration curve specific to CeO_2-NPs was employed for quantification. The acquisition parameters are detailed in Table S5. The mass concentrations of TiO_2-NPs and CeO_2-NPs in the TAP exposure medium were measured by SC-ICP-MS (Table S6) and showed good agreement with the nominal values.

The cells and possible NP aggregates were also visualized by a cell imaging multimode reader (Cytation 7 Image Reader, Biotek, Santa Clara, USA) with Gen 5 version 3.14 software.

2.6. Data analysis

To assess significant differences among treatment groups, a one-way analysis of variance (ANOVA) was conducted. Prior to performing ANOVA, the assumptions of normality were tested using the Shapiro–Wilk test. Tukey's Honestly Significant Difference (HSD) test was applied as a post hoc comparison to determine pairwise differences between means. Tukey's HSD was chosen for its balanced conservativeness and statistical power. All analyses were performed using OriginPro 2023 (v. 9.6.5.169; OriginLab Corporation, Northampton, MA, USA), and differences were considered statistically significant at $p < 0.05$. Agilent ICP-MS MassHunter Workstation software (Agilent, Morges, Switzerland) and Syngistix for ICP-MS software (Perkin Elmer, Perkin Elmer, Toronto, Canada) were used for data treatment.

3. Results and discussion

3.1. Characterization of TiO_2-NPs or CeO_2-NPs suspensions in exposure medium

SP-ICP-MS results showed that the most frequent size for TiO_2-NPs in TAP exposure medium was around 70–90 nm (limit of detection $(LOD)_{size}$ 44 nm) (Fig. 1a), which was larger than the values obtained in ultrapure water (Fig. S2a), suggesting that the components in the exposure medium promoted NPs aggregation. In contrast, CeO_2-NPs had a measured size of 50 nm (LOD_{size} 24 nm) (Fig. 1b), with no size dependence on NPs concentration. This differed from TiO_2-NPs, where larger aggregates formed as the initial NP concentrations increased. Additionally, the size of CeO_2-NPs was comparable to the one observed in ultrapure water (Fig. S2b), indicating that the medium did not significantly influence their aggregation. No dissolution for any of the NPs was found in the exposure medium, with dissolved element concentrations below the SP-ICP-MS LOD (5.14 ng L^{-1} for TiO_2-NPs and 1.44 ng L^{-1} for CeO_2-NPs).

DLS analysis showed pronounced aggregation of both TiO_2-NPs and CeO_2-NPs in the exposure medium, with the extent of aggregation increasing with the NPs concentration. For TiO_2-NPs, the z-average hydrodynamic size ranged from less than 0.1 μm at 0.1 mg L^{-1} to 1.8 μm at 50 mg L^{-1} (Fig. 1c). Similarly, for CeO_2-NPs, the size increased from 0.3 μm at 0.1 mg L^{-1} to 1.2 μm at 50 mg L^{-1} (Fig. 1d). The observed zeta potential values were negative, measuring −9.49 ± 2.37 mV for TiO_2-NPs and −6.55 ± 2.30 mV for CeO_2-NPs. TiO_2-NPs are known to aggregate more readily in the presence of Ca^{2+} and Mg^{2+} in TAP medium due to lower colloidal stability (Domingos et al., 2010; Xu, 2018), making them particularly susceptible to overestimation in DLS. Both NPs have surfaces that readily adsorb phosphate, carbonate (Connor and

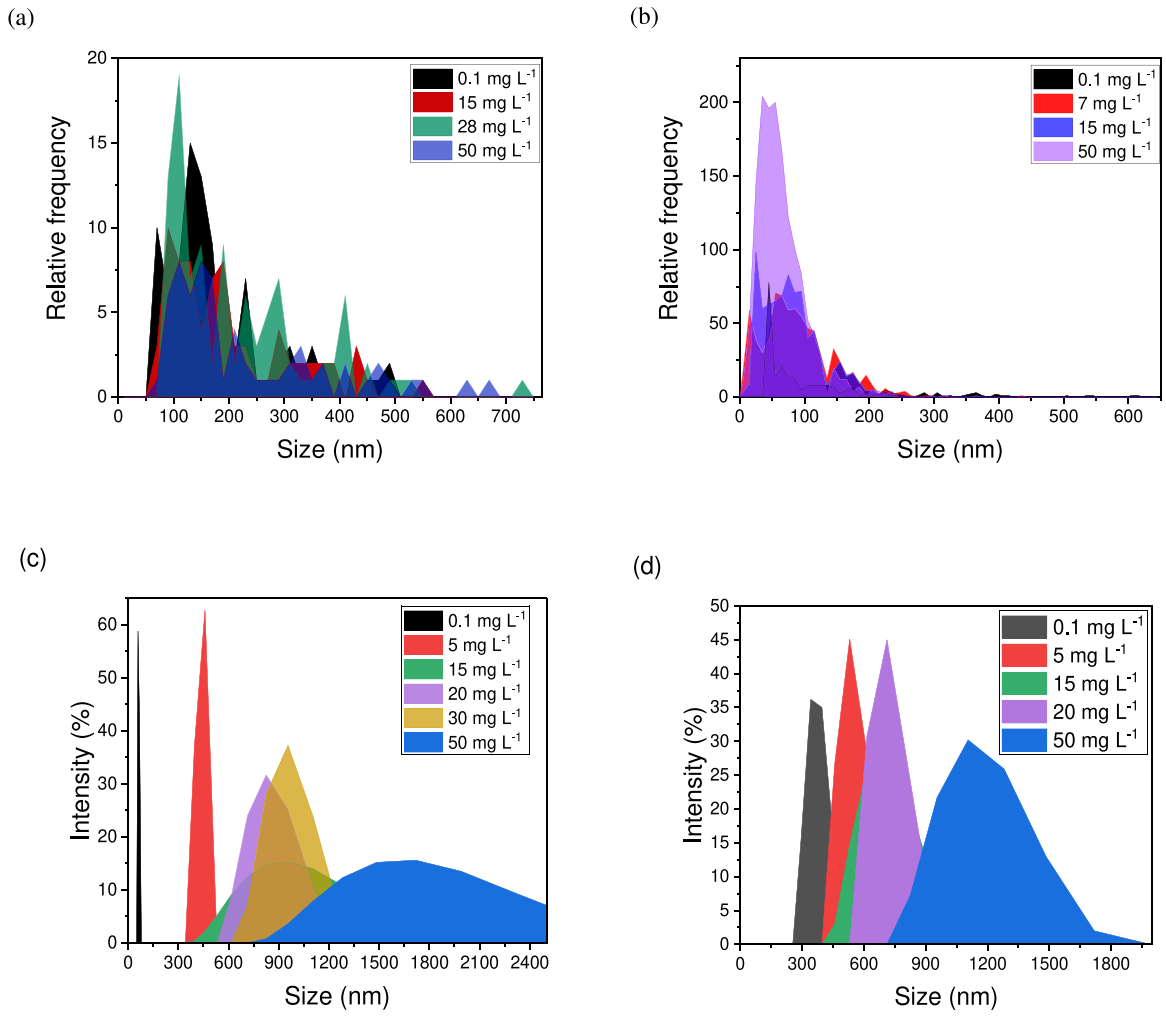

Fig. 1. Size distributions obtained by SP-ICP-MS for the suspensions of (a) TiO_2-NPs and (b) CeO_2-NPs. Hydrodynamics size distributions found by DLS for the suspensions of (c) TiO_2-NPs and (d) CeO_2-NPs. Exposure medium TAP, pH 7.0 and exposure time of 72 h.

McQuillan, 1999; Hu et al., 2025) also present in the exposure medium. However, SP-ICP-MS revealed greater aggregation of TiO_2-NPs compared to CeO_2-NPs in the exposure medium. Despite TiO_2-NPs having a slightly more negative zeta potential, both materials showed weak electrostatic repulsion, suggesting other factors drive the aggregation. Differences in surface chemistry, hydration layers, and oxide properties likely play a role, TiO_2-NPs especially anatase, has higher surface energy, promoting aggregation, while CeO_2-NPs are redox-active (Mohajeri et al., 2025).

DLS measurements yielded larger sizes compared to those obtained by SP-ICP-MS. This difference arises because SP-ICP-MS provides the nominal particle size, whereas DLS measures the hydrodynamic size, which accounts for the nanoparticle's interaction with the surrounding medium, leading to higher values. Additionally, the dilution required for SP-ICP-MS analysis may have caused partial disaggregation of the NPs, further contributing to the smaller sizes observed with this technique. Nevertheless, both techniques confirmed the significant aggregation in the exposure medium, as the primary particle sizes reported by JRC through transmission electron microscopy (TEM) were 22 nm, with aggregates ranging from 20 to 500 nm for TiO_2-NPs (Rasmussen et al., 2014) and 28 nm, with aggregates of approximately 100 nm for CeO_2-NPs (Singh et al., 2014).

3.2. Effect of TiO_2-NPs and CeO_2-NPs on algal growth

Both TiO_2-NPs and CeO_2-NPs inhibited the growth of *R. subcapitata* in a concentration-dependent manner (Fig. 2). However, the EC_{50} value slightly decreased when exposure time increased from 24 h (16.2 ± 0.4 mg L^{-1} for TiO_2-NPs and 7.92 ± 0.58 mg L^{-1} for CeO_2-NPs) to 72 h (28.3 ± 1.16 mg L^{-1} for TiO_2-NPs and 13.6 ± 0.57 mg L^{-1} for CeO_2-NPs). This shift was more pronounced for TiO_2-NPs. This decrease may result from a combination of physicochemical and biological factors. Studies have shown that attachment parameters, strongly influenced by the nanoparticle-to-cell ratio in short-term exposures, can serve as predictors of CeO_2-NPs and TiO_2-NPs toxicity (Hund-Rinke et al., 2020). For 48 h, the EC_{50} obtained were 27.0 ± 0.10 mg L^{-1} for TiO_2-NPs and 13.7 ± 0.90 mg L^{-1} for CeO_2-NPs. These values are comparable to the values obtained for 72 h exposure. The increased aggregation over longer exposure durations, coupled with the sedimentation of larger aggregates, may reduce the number of NPs and aggregates available to interact with the algal surface, stabilizing the toxicity effects. Furthermore, as microalgae grow during the exposure period, the changing cell-to-nanoparticle ratio may further influence the dynamics of their interactions.

The 72 h-EC_{50} values were 28.3 ± 1.16 mg L^{-1} for TiO_2-NPs and 13.6 ± 0.57 mg L^{-1} for CeO_2-NPs, indicating about twice the higher toxicity of CeO_2-NPs than TiO_2-NPs. These observations align with existing literature on various phytoplankton species, confirming that CeO_2-NPs exhibit higher toxicity than TiO_2-NPs (Cerrillo et al., 2016; Hund-Rinke et al., 2020). Similar trends have been reported for *R. subcapitata*, with 72 h-EC_{50} values of 10.9 and 126.9 mg L^{-1} for CeO_2-NPs and TiO_2-NPs in OECD medium (Hund-Rinke et al., 2020). Additionally, 72 h-EC_{50} of

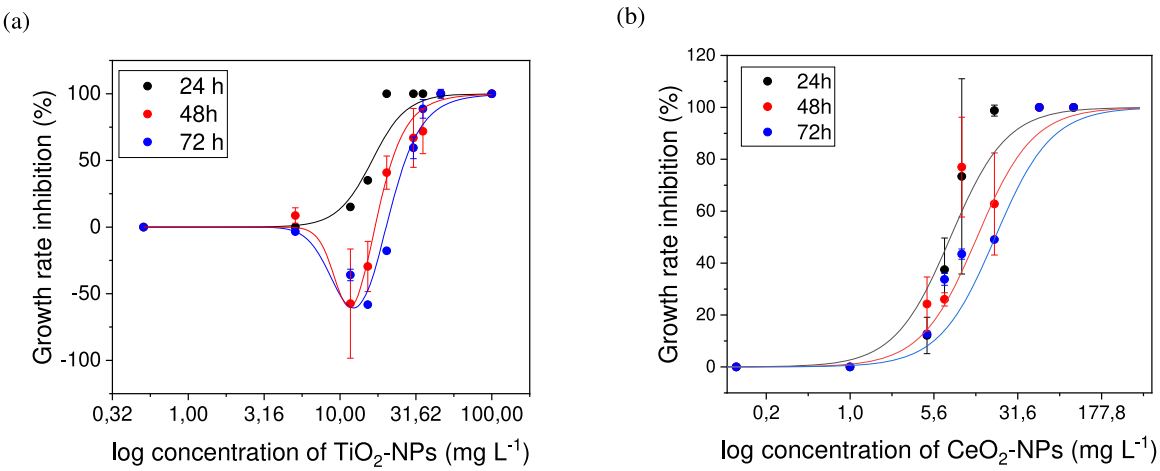

Fig. 2. Growth inhibition curves for *R. subcapitata* exposed to increasing concentrations of TiO_2-NPs (a) and CeO_2-NPs (b) at 24 h, 48 h and 72 h exposure. The fitting for TiO_2-NPs followed the equation proposed by (Deng et al., 2012), the fitting for CeO_2-NPs was performed using the Hill equation ($n = 3$). The exposure concentration is present in log-scale.

7.6 and 59 mg L^{-1} for 10 and 34 nm for CeO_2-NPs were reported in synthetic freshwater (Angel et al., 2015). For other algal species, higher 72 h-EC_{50} values have been observed in the literature. In *C. reinhardtii*, TiO_2-NPs of 5, 15, and 20 nm required concentrations exceeding 200 mg L^{-1} to achieve 50 % growth inhibition (Liu et al., 2022). In the marine microalga *Tetraselmis suecica*, the 72h-EC_{50} was 106.26 mg L^{-1} for 10–25 nm TiO_2-NPs (Bameri et al., 2023). For CeO_2-NPs, a 96-h exposure to 48 nm NPs resulted in an EC_{50} of 176.3 mg L^{-1} (Angel et al., 2015).

Interestingly, exposure to TiO_2-NPs induced a biphasic response in *R. subcapitata*, with both stimulatory and inhibitory phases observed, indicating a hormesis response of this algae, already at 48 h of exposure. No such biphasic response was observed for this alga exposed to CeO_2-NPs over the tested concentration range. The stimulatory phase was observed in the concentration range from 10 to 20 mg L^{-1} TiO_2-NPs (Fig. 2a) and reached a stimulation maximum in 60 % of cells at 13 mg L^{-1} TiO_2-NPs after 72 h. Such strong growth stimulation at intermediate concentrations is seldom reported and often overlooked in ecotoxicology. These findings align with the literature, where a hormesis effect was previously reported for 25 nm TiO_2-NPs at concentrations between 16 and 20 mg L^{-1} for *R. subcapitata* (Nogueira et al., 2015). Biphasic dose responses have been reported across various organisms and different types of NPs (Agathokleous et al., 2022), including microalgae (Agathokleous et al., 2019; Huang et al., 2022). For instance, low concentrations of TiO_2-NPs (< 100 nm) have been shown to stimulate growth in cyanobacterium *M. aeruginosa* (Wu et al., 2019). Similarly, CeO_2-NPs of 26 nm induced hormesis effects on the cell density of C. reinhardtii and Phaeodactylum tricornutum at concentrations between 10 and 100 mg·L^{-1} after 72 h of exposure, while CeO_2-NPs of 9 nm reduced cell density, aligning with the findings of this study (Sendra et al., 2017). The factors driving the hormesis response in algae remain largely unexplored. However, the accumulation of ROS, the production of antioxidant metabolites, and the increased activity of antioxidant enzymes are considered key contributors (Agathokleous et al., 2019, 2022).

3.3. Interactions of TiO_2-NPs and CeO_2-NPs aggregates with algae

Both NPs and their aggregates were attached to the cell surface and formed hetero-aggregates as shown in the brightfield microscopy images (Fig. 3). The number of NPs and their aggregates adsorbed to algal surface increased with NP concentration for both TiO_2-NPs and CeO_2-NPs. At 0.5 mg L^{-1}, no particles were observed attached to the cells after 72 h of exposure. However, at higher concentrations, particles were seen surrounding the cells, and at 50 mg L^{-1}, cells were completely covered by NPs. This pattern was more pronounced at the highest CeO_2-NPs concentration. These findings suggest a threshold effect, where higher particle concentrations favor non-specific associations due to more frequent collisions. At elevated concentrations, NPs tend to aggregate, forming large clusters that can physically trap or settle onto algal surfaces, pointing to a mechanism driven mainly by particle–particle interactions. However, initial contact with algal cells may also trigger aggregation, suggesting a combined role of cell–particle and particle–particle interactions. The significant increase in ROS generation, especially in CeO_2-NPs treatments, further implies that passive entrapment alone doesn't explain the effects. Since oxidative stress typically requires close contact, biologically relevant surface interactions likely contribute to these interactions. The dependence of hetero-aggregation on NPs concentration has also been reported in the literature for 5–30 nm TiO_2-NPs in *R. subcapitata* (Rivero Arze et al., 2020; Skjolding et al., 2022) and *Microcystis aeruginosa* (Wang et al., 2024). Similarly, exposure to 25 nm CeO_2-NPs resulted in hetero-aggregation in cyanobacterium *Prochlorococcus* sp. (Dedman et al., 2021) and 10 –30 nm CeO_2-NPs in *Phaeodactylum tricornutum* (Deng et al., 2017). The formation of these hetero-aggregates can reduce the availability of light and nutrients to algae due to the shading effect (Ghazaei and Shariati, 2020; Hund-Rinke et al., 2020; Xia et al., 2015) and thus via physical effect to contribute to the algal growth inhibition.

In addition, the adsorption of uncoated 10–60 nm CeO_2-NPs with *R. subcapitata* and cyanobacterium *Anabaena* caused superficial damage, leading to cell wall and membrane disruption (Rodea-Palomares et al., 2011).

3.4. Effect of TiO_2-NPs and CeO_2-NPs on cellular granularity and chlorophyll fluorescence

The interaction of TiO_2-NPs and CeO_2-NPs with algal cells led to an increase in cell granularity (Fig. S3), as determined by comparing the mean SSC by FCM of the unexposed and exposed to NPs cell populations. Elevated SSC typically reflects greater internal structural complexity, often due to NP internalization within the cytoplasm (Zucker et al., 2010). An increase in granularity might indicate that NPs are being adsorbed and/or internalized into the algal cells (Manier et al., 2013; Rivero Arze et al., 2020; Zucker et al., 2010). At a concentration of 0.5 mg L^{-1}, TiO_2-NPs altered the granularity of 60 % of cells, which further increased to 94 % at 10 mg L^{-1} compared to unexposed cells. For CeO_2-NPs, exposure to 1 mg L^{-1} resulted in a change of granularity of 23 % of the cells, which increased to 76 % at 5 mg L^{-1}. At the highest tested concentration of 50 mg L^{-1}. For CeO_2-NPs, granularity changes reached

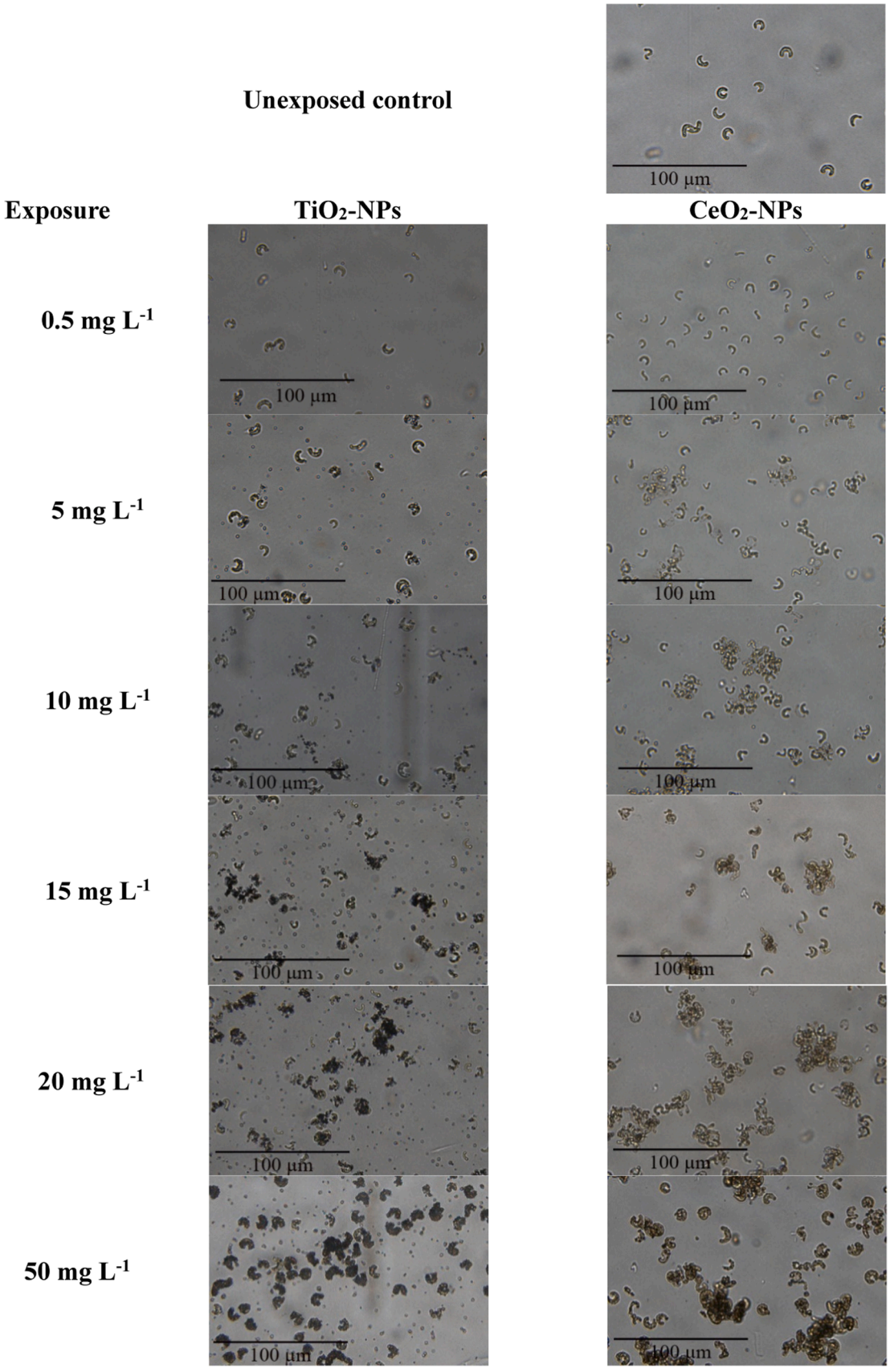

Fig. 3. Brightfield images for *R. subcapitata* exposed to increasing concentrations of TiO_2-NPs and CeO_2-NPs for 72 h.

97 %, a level like that observed for TiO_2-NPs. These findings are consistent with literature reporting that TiO_2-NPs induced an 80 % increase in granularity at 10 mg L^{-1} when using the OECD medium (Rivero Arze et al., 2020). Changes in SSC and forward side scatter (FSC) were also observed for *Nitzschia closterium,* with TiO_2-NPs uptake confirmed by SEM (Xia et al., 2015). Similarly, alterations in cell complexity were reported for Chlamydomonas reinhardtii, Phaeodactylum tricornutum, and Nannochloris atomus following exposure to <25 nm and 30–50 nm CeO_2-NPs (Sendra et al., 2017). These changes depended on NP size and surface charge, with a more pronounced effect for positively charged NPs. However, in the present study, both CeO_2-NPs and TiO_2-NPs were negatively charged, which suggests that electrostatic interactions are not the main drivers. In addition, other forces involved in the adsorption onto the algal surface, such as van der Waals forces, hydrophobic interactions, and specific chemical interactions including hydrogen bonding and receptor–ligand binding (Liu, 2021; Slaveykova et al., 2020; von Moos et al., 2015), may play a more significant role.

A slight shift in the chlorophyll fluorescence distribution was observed when algae were exposed to TiO_2-NPs or CeO_2-NPs at concentrations above 5 mg L^{-1} (Fig. S4). Given the notable changes in cellular granularity, particularly at higher exposure concentrations, we closely examined chlorophyll fluorescence in cells exhibiting altered granularity. In this subpopulation, a pronounced shift in chlorophyll fluorescence towards higher values was detected under TiO_2-NPs exposure (Fig. S5). A similar shift was observed with CeO_2-NPs exposure, accompanied by distribution broadening and a decrease in intensity of the distribution maximum (Fig. S6). In contrast, no significant changes in chlorophyll fluorescence were detected in cells with unaffected or minimally affected granularity. These results suggest that the increase in chlorophyll fluorescence is associated with NPs-induced changes in cellular granularity. In addition, metal oxide NPs are known to induce oxidative stress in algae by directly generating ROS at their surfaces and by interfering with photosynthetic electron transport (von Moos and Slaveykova, 2014). In our study, the agglomeration of NPs likely enhanced their interaction with algal cells, as larger NP clusters can settle more readily onto cell surfaces and create localized microenvironments with higher effective NP concentrations. This, in turn, can lead to elevated ROS production in close proximity to or within the cells. As a result, algal cells associated with larger NP agglomerates may experience increased oxidative stress, leading to more pronounced shifts in pigment composition—namely, increased carotenoids, decreased chlorophyll, and the expression of other stress-responsive pigments.

In the literature, enhanced chlorophyll a fluorescence has been reported for *R. subcapitata* (Mahaye and Musee, 2023) and *C. reinhardtii* (Pulido-Reyes et al., 2019), attributed to NPs effect on the acceptor side of photosystem II. Conversely, a decrease in chlorophyll fluorescence was observed following CeO_2-NPs exposure in *C. vulgaris* and *Chlorella pyrenoidosa* (Liu et al., 2024; Xie et al., 2021). In *Microcystis aeruginosa*, exposure to 25 nm TiO_2-NPs induced changes in chlorophyll *a* that varied with exposure duration. Photosynthetic activity was inhibited, likely due to light shading caused by TiO_2-NPs adsorbed on the cell surface (Wang et al., 2024). Additionally, disturbances in the photosynthetic system were associated with elevated chlorophyll *b* content, likely triggered by NPs exposure, which in turn led to the generation of ROS (Liu et al., 2024).

3.5. Effect of TiO_2-NPs and CeO_2-NPs on ROS generation and membrane damage

ROS generation has been identified as a key mechanism of NP toxicity (Liu et al., 2024; von Moos and Slaveykova, 2014; Wang et al., 2024; Xie et al., 2021). Exposure to increasing concentrations of TiO_2-NPs or CeO_2-NPs resulted in enhanced ROS generation compared to unexposed cells (Fig. 4a). At exposure concentrations below 1 mg L^{-1} TiO_2-NPs induced mild but a greater increase in ROS generation than CeO_2-NPs (Fig. 4a). In the concentration range between 10 and 20 mg L^{-1} TiO_2-NPs, the cellular ROS generation was about 20 % and did not change with the concentrations, suggesting that the antioxidant systems can cope with the enhanced ROS generation (von Moos and Slaveykova, 2014). At concentrations higher than 15 mg L^{-1}, CeO_2-NPs exhibited a more potent ROS-generating effect (57.3 ± 1.2 %) than TiO_2-NPs (18.6 ± 8.2 %). For example, at the highest tested concentration of 50 mg L^{-1}, cellular ROS generation was significantly higher for CeO_2-NPs (71.8 ± 1.2 %) compared to TiO_2-NPs (39.5 %). These results suggest that the antioxidant defense system is overwhelmed in algae when exposed to high CeO_2-NPs concentration. The above trends are consistent with growth inhibition results, as CeO_2-NPs demonstrated a lower 72h-EC_{50} value than TiO_2-NPs (Fig. 2), as well as with the results for the cellular membrane damage observed at 50 mg L^{-1} CeO_2-NPs (Fig. 4b). Furthermore, the NPs aggregation can significantly influence oxidative stress and damage in algae by reducing the surface area available for cell interaction (Xu, 2018). Since ROS TiO_2-NPs induced ROS production is particle surface-mediated and photocatalytic, aggregation can decrease ROS output per unit mass (Wang et al., 2024).

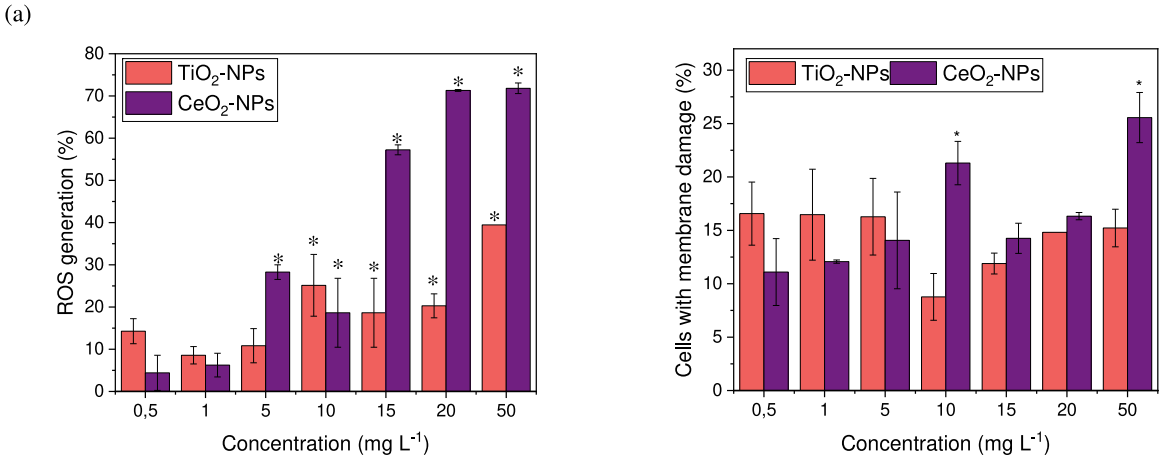

Fig. 4. (a) ROS generation in *R. subcapitata* exposed to increasing concentrations of TiO_2-NPs and CeO_2-NPs for 72 h. Data are present as % of the increase of ROS generation in comparison with unexposed control. The asterisks indicate a significant difference between the exposure concentrations, as obtained by one-way ANOVA followed by a Tukey test ($p < 0.05$, $n = 3$, degrees of freedom, DF=7, F-value=15.8). (b) Percentage of cells with membrane damage obtained for the exposure to TiO_2-NPs and CeO_2-NPs for 72 h. The asterisks indicate a significant difference between the exposure concentrations, as obtained by one-way ANOVA followed by a Tukey test ($p < 0.05$, $n = 3$, degrees of freedom, DF = 13, F-value = 5.4).

In the present study, TiO_2-NPs aggregated more than CeO_2-NPs at the same exposure concentrations and generated less ROS. CeO_2-NPs may produce more ROS due to their redox cycling between Ce^{3+} and Ce^{4+}, though this antioxidant activity depends on surface accessibility and the Ce^{3+}/Ce^{4+} ratio, both of which can be reduced by aggregation (Mohajeri et al., 2025).

A similar increase in the ROS generation at high concentration of 21 nm TiO_2-NPs has been reported in the literature for *Chlorella* sp. (Thiagarajan et al., 2021) and *Dunaliella salina* (Thiagarajan et al., 2019). However, for *Phaeodactylum tricornutum* (Wang et al., 2016) and *C. pyrenoidosa* (Zhu et al., 2022), intracellular ROS levels were not significantly different from the control at concentrations of 10 and 50 mg L^{-1} of TiO_2-NPs after 96 h exposure, indicating that the effects are algal species dependent. Exposure of *C. reinhardtii* to increasing concentrations of TiO_2-NPs with primary sizes of 5, 15 and 20 nm resulted in a NPs-size dependent excessive generation of cellular ROS, which was more pronounced for the 5 nm TiO_2-NPs (Liu et al., 2022). In cyanobacterium *M. aeruginosa*, an increase in malondialdehyde (MDA) and catalase (CAT) activity was observed due to ROS accumulation after the exposure to 25 nm TiO_2-NPs, starting at concentration of 1 mg L^{-1} (Wang et al., 2024). The activities of superoxide dismutase, catalase and peroxidase also increased after 2 h of exposure to TiO_2-NPs due to the excessive generation of ROS (Xia et al., 2015). However, the present results somewhat contradict previous findings. For *C. reinhardtii* exposed to 10 mg L^{-1} of uncoated CeO_2-NPs, no ROS generation was reported. In contrast, greater ROS levels were observed for PVP-coated NPs. Interestingly, despite the lower number of uncoated NPs detected inside the cells compared to PVP-coated NPs, the uncoated NPs caused more damage to the cell membrane (Pulido-Reyes et al., 2019).

Exposure to increasing concentrations of TiO_2-NPs or CeO_2-NPs led to a mild increase in the proportion of the cells with compromised membranes in comparison with the unexposed cells (Fig. 4b). There was no concentration dependence on TiO_2-NPs exposure, where the percentage of exposed cells with damaged membranes was around 15.0 - 16.6 %. Exposure to CeO_2-NPs led to a concentration-dependent increase in the percentage of cells with damaged membranes, ranging from 11.0 % at 0.5 mg L^{-1} to 25.6 % at 50 mg L^{-1}. This increase in the cells with damaged membranes is consistent with the enhanced ROS generation by CeO_2-NPs, which could lead to lipid membrane peroxidation, as observed previously in *R. subcapitata* (Ozkaleli and Erdem, 2018) and other green algae, such as *C. reinhardtii* (Pulido-Reyes et al., 2019), *C. vulgaris* (Liu et al., 2024) and *C. pyrenoidosa* (Xie et al., 2021). In *C. reinhardtii*, exposure to 5 nm TiO_2-NPs caused a significant increase in the percentage of cells with membrane damage at much higher

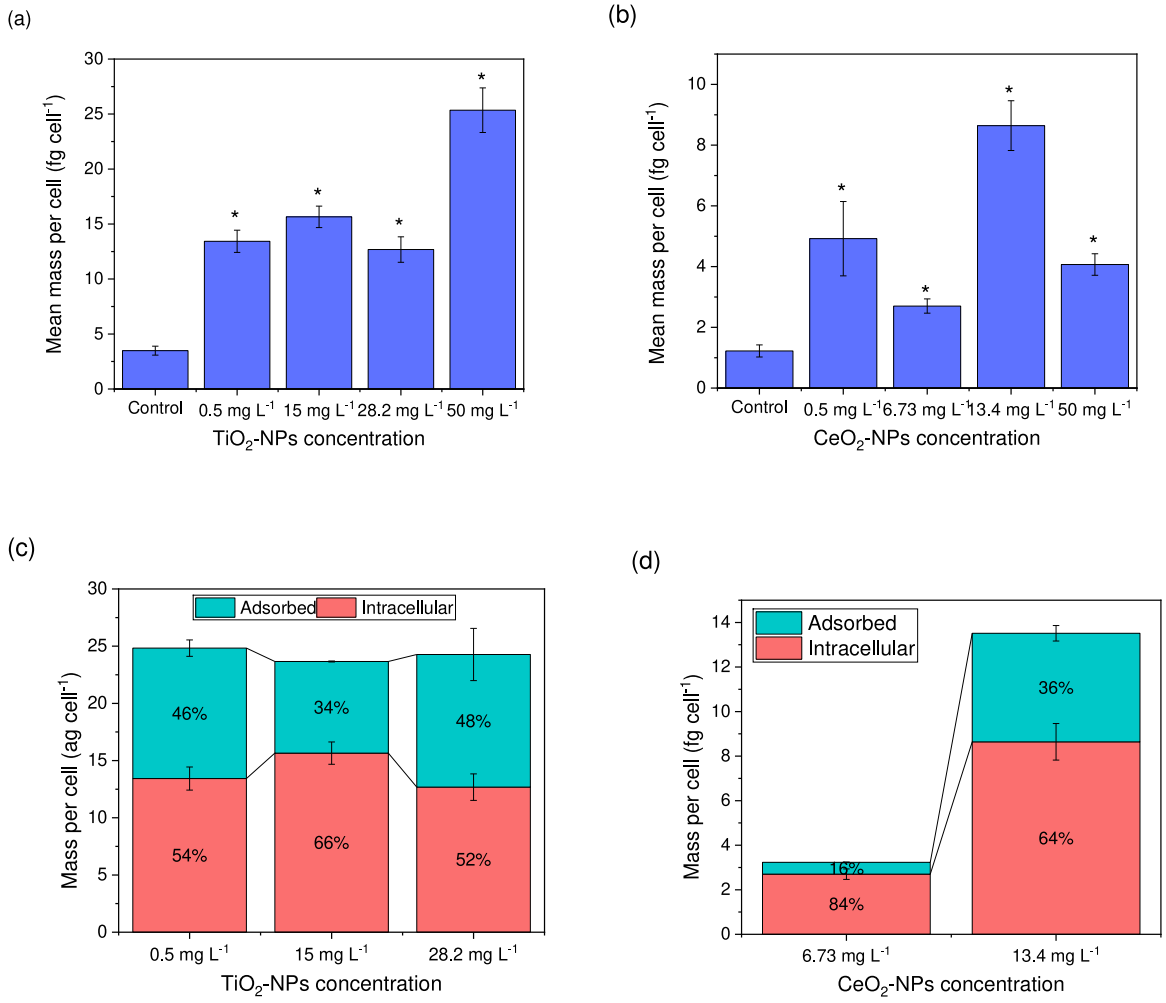

Fig. 5. Uptake of titanium and cerium by algae measured using SC-ICP-MS. (a) Mean intracellular mass of Ti per cell after the EDTA washing cycle. The asterisks indicate a significant difference between the exposure concentrations and the control, as obtained by one-way ANOVA followed by a Tukey test ($p < 0.05$, $n = 3$, degrees of freedom, DF = 3, F-value = 55.3). (b) Mean intracellular mass of Ce per cell after the EDTA washing cycle. The asterisks indicate a significant difference between the exposure concentrations and the control, as obtained by one-way ANOVA followed by a Tukey test ($p < 0.05$, $n = 3$, degrees of freedom, DF = 3, F-value = 26.1). (c) Mean total cellular mass of Ti per cell without EDTA washing and distribution between intracellular (EDTA non extractable) and adsorbed fractions. (d) Mean total cellular mass of Ce per cell without EDTA washing and distribution between intracellular (EDTA non extractable) and adsorbed fractions.

concentrations (200 mg L^{-1}). In contrast, for 15 nm and 20 nm TiO_2-NPs, the percentage of cells with membrane damage was very low and comparable to that of unexposed controls (Liu et al., 2022).

3.3. Uptake of TiO_2-NPs and CeO_2-NPs by R. subcapitata

The uptake of TiO_2-NPs and CeO_2-NPs was characterized by Ti and Ce content per cell, as determined by SC-ICP-MS (Fig. 5). EDTA washing was used to distinguish operationally between intracellular (EDTA-non extractable) and adsorbed (EDTA-extractable) metal content. We suggest that in the EDTA-washed treatment, NPs adsorbed to the algal surface were likely removed via chelation of divalent cations, such as Ca^{2+} and Mg^{2+}, which play a critical role in maintaining the integrity of the algal cell wall matrix. Their removal may weaken the matrix structure, thereby facilitating the detachment of bound NPs. As the SP-ICP-MS results showed no release of Ti or Ce ions from the NPs, we can attribute the cellular metal content to the NPs uptake. Exposure to TiO_2-NPs at concentrations of 0.5 and 15 mg L^{-1} resulted in no significant differences in the intracellular fraction, with the elemental mass per cell remaining around 14 fg of Ti (Fig. 5a). However, at 28 and 50 mg L^{-1}, a shift toward higher intracellular Ti masses was observed (Fig. S7a), reaching 24 fg of Ti per cell at 50 mg L^{-1}. At the concentration of 28.3 mg L^{-1} TiO_2-NPs corresponding to 72h-EC_{50}, it was about 12.5 fg of Ti per cell. The SC-ICP-MS analysis of the cells without the EDTA washing cycle revealed that for TiO_2-NPs, cellular Ti content (adsorbed + intracellular) was comparable for the exposure between 0.5 and 28.2 mg L^{-1}. The percentage of adsorbed Ti remained relatively constant at 46–48 % regardless of NPs concentration, too (Fig. 5c). In previous studies, an increase in intracellular Ti was observed with rising concentrations (Thiagarajan et al., 2021, 2019). However, those studies measured the total internalized titanium concentration rather than the titanium content per individual cell, as done in this study.

For CeO_2-NPs, lower values of the mass of the element per cell than for TiO_2-NPs in the intracellular fraction were observed (Fig. 5b). For the lowest concentrations of 0.5 mg L^{-1} CeO_2-NPs, there were no significant differences between the mass of Ce per cell (approximately 5 fg per cell). For the concentration which corresponds to the EC_{50} (13 mg L^{-1}), the Ce mass in the intracellular fraction increased to 9 fg per cell. The intracellular Ce content further decreased to 4 fg per cell at 50 mg L^{-1}. This reduction at CeO_2-NPs high concentration may be attributed to significant cell membrane damage under these conditions (Fig. 4b), which could promote NPs release from damaged cells. Increasing exposure concentration from 6.73 to 13.4 mg L^{-1} resulted in a rise in total cellular Ce content from 3 to 13 fg Ce per cell. In addition, the proportion of Ce adsorbed per cell increased from 16 % to 36 % as the exposure concentration increased (Fig. 5d). Therefore, measured mass cellular concentration should be taken with caution, especially at high NP concentrations, where membrane-damaged cells may accumulate NPs due to impaired metabolism, failed active transport, or aggregation, or may instead lose them more easily.

These findings are consistent with literature reports showing the presence of NPs in algal cells (Ghazaei and Shariati, 2020; Li et al., 2015; Middepogu et al., 2018; Thiagarajan and Ramasubbu, 2022; Xia et al., 2015). Titanium particles were found attached to the cell walls and accumulated inside the chloroplast of the alga *Karenia brevis* (Li et al., 2015). Similarly, interactions with mitochondria and chloroplast have been observed in diatoms *Dunaliella salina* and *D. tertiolecta* after exposure to 25–30 nm TiO_2-NPs (Ghazaei and Shariati, 2020), as well as damage to the thylakoid system of chloroplasts for *C. pyrenoidosa* following exposure to 12 nm TiO_2-NPs (Middepogu et al., 2018). 21 nm TiO_2-NPs has also been observed inside *Nitzschia closterium* using TEM (Xia et al., 2015), in *Chlorella* sp. exposed to 26 nm-sized TiO_2-NPs (Thiagarajan and Ramasubbu, 2022) and *C. pyrenoidosa* (Zhu et al., 2022).

Regarding CeO_2-NPs, the present study is the first one reporting an increase in the intracellular Ce per cell upon CeO_2-NPs exposure, as no internalization has been previously reported for green algae *R. subcapitata* (Mackevica et al., 2023; Manier et al., 2013) and *C. reinhardtii* (Kosak Nee Rohder et al., 2018). In contrast, for *C. reinhardtii*, internalization of uncoated 4 nm CeO_2-NPs has been observed and presumed to be due to cell wall damage, allowing direct membrane transport (Pulido-Reyes et al., 2019). When coated with PVP, CeO_2-NPs entered cells via endocytosis without causing membrane damage (Pulido-Reyes et al., 2019; Taylor et al., 2016). The present study was not designed to investigate the uptake mechanisms of TiO_2-NPs and CeO_2-NPs. However, based on existing literature, particles smaller than 100 nm are suggested to enter cells via endocytosis or by penetrating the membrane following membrane damage. To the best of our knowledge, however, endocytosis uptake pathways have not yet been demonstrated for this algal species.

Both TiO_2-NPs and CeO_2-NPs aggregate with microalgae, absorb on the surface and internalize into cells, leading to physical and ROS-induced damage to the cell membrane, which resulted in the alteration of microalgal growth. The adsorption and direct contact of NPs with algae, along with their potential penetration (or lack thereof) through biological membranes, are considered prerequisites for toxicity (Mahana et al., 2021; von Moos et al., 2014; Yu et al., 2025). The results of the study challenge the assumption that higher NP uptake correlates directly with greater toxicity, as TiO_2-NPs showed higher accumulation in cells than CeO_2-NPs, yet CeO_2-NPs induced stronger oxidative stress and growth inhibition. This decoupling of uptake and toxicity provides new evidence suggesting that surface reactivity and redox behavior—not just internalization—are critical to NPs toxicity in alga. This observation suggests that key paradigms established for dissolved pollutants - such as the biotic ligand model or critical body concentration (Vijver et al., 2018), which assume that a higher concentration of a pollutant inside cells correlates with greater toxic potential - are not directly applicable to these NPs and algae. However, the aggregate NPs, while not typically considered part of the bioavailable fraction, may still serve as a source of individual particles that can be released and potentially contribute to toxicity.

The findings of this laboratory study may have important implications for contaminated aquatic environments. As microalgae represent the foundation of aquatic food webs, any negative impacts on their health could lead to cascading effects on higher trophic levels, including herbivorous zooplankton. SC-ICP-MS analysis revealed that the cellular Ti content was approximately twice as high as that of Ce at comparable exposure concentrations (e.g. 15 mg L^{-1}). This suggests that TiO_2-NPs may be more readily transferred to primary consumers through trophic interactions. Moreover, given the significant surface attachment of NPs aggregates to the algal cells, this adsorbed fraction could also play a crucial role in nanoparticle transfer via predation in the food web, as previously suggested (Geitner et al., 2016).

The results of the present study confirmed that exposure to TiO_2-NPs and CeO_2-NPs at concentrations higher than those typically found in natural waters (Azimzada et al., 2021) can induce oxidative stress, cause membrane damage, and ultimately lead to a decrease in algal growth. Such effects on microalgae could have serious implications for primary productivity in strongly contaminated aquatic environments. As microalgae are key primary producers, their reduced growth and photosynthetic efficiency may lower the overall rate of carbon fixation and oxygen production. This decline in primary productivity could, in turn, impact nutrient cycling, energy flow, and the availability of food for higher trophic levels.

4. Conclusions

This study uniquely integrates state-of-the-art single-entity techniques—FCM, SC-ICP-MS, and SP-ICP-MS—to provide a comprehensive, high-resolution assessment of TiO_2-NPs and CeO_2-NPs toxicity in the green alga *R. subcapitata*, capturing interactions at the level of individual particles and cells. The study revealed that both TiO_2-NPs and CeO_2-NPs

exert dose-dependent growth inhibition, with CeO_2-NPs showing greater toxicity. TiO_2-NPs exhibited a hormesis response at intermediate concentrations and induced moderate oxidative stress, whereas CeO_2-NPs led to a stronger increase in ROS, particularly at higher exposure concentrations. SC-ICP-MS confirmed that both types of nanoparticles were adsorbed and internalized by algal cells, with Ti generally accumulating to higher levels than Ce. However, the uptake of CeO_2-NPs increased more markedly with exposure. SP-ICP-MS showed no detectable ion release, indicating that the observed cellular metal content resulted from particulate uptake. Importantly, the extent of internalization did not directly correlate with toxicity, suggesting that nanoparticle surface reactivity and redox properties play a more decisive role in biological outcomes. The greater impact of CeO_2-NPs, despite lower cellular accumulation, highlights the significance of redox-active surfaces as drivers of adverse effects. This decoupling of uptake from response marks a critical advancement in nanoecotoxicology and highlights the need to evaluate different aspects of the NPs-cell interactions. These findings demonstrate the value of high-resolution, single-entity analytical techniques in advancing our understanding of NPs–alga interactions and impacts in aquatic ecosystems.

CRediT authorship contribution statement

Mariam Bakir: Writing – original draft, Validation, Methodology, Investigation, Formal analysis, Conceptualization. **Isabel Abad-Alvaro:** Writing – review & editing, Validation, Methodology. **Francisco Laborda:** Writing – review & editing, Validation, Supervision, Funding acquisition. **Vera I. Slaveykova:** Writing – review & editing, Validation, Supervision, Funding acquisition, Conceptualization.

Declaration of competing interest

The authors declare that they have no known competing financial interests or personal relationships that could have appeared to influence the work reported in this paper.

Funding

This work received financial support from Lead Agency Swiss National Science Foundation/ US National Science Foundation Grant N° 10000227, the Spanish Ministry of Science and Innovation (MCIN/AEI/10.13039/501100011033), project PID2021–123203OB-I00, "ERDF A way of making Europe" and the Government of Aragon, project E29_23R.

Acknowledgements

The authors would like to acknowledge the European Commission Joint Research Centre Nanomaterials Repository for providing the nanomaterials and the use of the Servicio General de Apoyo a la Investigación-SAI, Universidad de Zaragoza. I.A. thanks the European Union-Next Generation EU and the Spanish Ministry of Universities for funding under the María Zambrano Grant (MZ-240621).

Supplementary materials

Supplementary material associated with this article can be found, in the online version, at doi:10.1016/j.aquatox.2025.107430.

Data availability

Data for this article, including NP characterization by SP-ICP-MS, effect of the NPs on algae obtained by FCM and biouptake determined by SC-ICP-MS are available at YARETA at https://doi.org/10.26037/yareta:lqze2mcuurdntahzxehoyslqxe.

References

Agathokleous, E., Feng, Z.Z., Iavicoli, I., Calabrese, E.J., 2019. The two faces of nanomaterials: a quantification of hormesis in algae and plants. Env. Int 131. https://doi.org/10.1016/j.envint.2019.105044.

Agathokleous, E., Wang, Q., Iavicoli, I., Calabrese, E.J., 2022. The relevance of hormesis at higher levels of biological organization: hormesis in microorganisms. Curr. Opin. Toxicol. 29, 1–9. https://doi.org/10.1016/j.cotox.2021.11.001.

Altammar, K.A., 2023. A review on nanoparticles: characteristics, synthesis, applications, and challenges. Front. Microbiol. 14, 1155622. https://doi.org/10.3389/fmicb.2023.1155622.

Angel, B.M., Vallotton, P., Apte, S.C., 2015. On the mechanism of nanoparticulate CeO_2 toxicity to freshwater algae. Aquat. Toxicol. 168, 90–97. https://doi.org/10.1016/j.aquatox.2015.09.015.

Azimzada, A., Jreije, I., Hadioui, M., Shaw, P., Farner, J.M., Wilkinson, K.J., 2021. Quantification and characterization of Ti-, Ce-, and Ag-nanoparticles in global surface waters and precipitation. Env. Sci. Technol. 55 (14), 9836–9844. https://doi.org/10.1021/acs.est.1c00488.

Bakir, M., Jimenez, M.S., Laborda, F., Slaveykova, V.I., 2024. Exploring the impact of silver-based nanomaterial feed additives on green algae through single-cell techniques. Sci. Total Env. 939, 173564. https://doi.org/10.1016/j.scitotenv.2024.173564.

Bameri, L., Sourinejad, I., Ghasemi, Z., Fazelian, N., 2023. Toxicological impacts of TiO_2 nanoparticles on growth, photosynthesis pigments, and protein and lipid content of the marine microalga *Tetraselmis suecica*. Bull. Env. Contam. Toxicol. 111 (3), 29. https://doi.org/10.1007/s00128-023-03782-w.

Bundschuh, M., Filser, J., Luderwald, S., McKee, M.S., Metreveli, G., Schaumann, G.E., Schulz, R., Wagner, S., 2018. Nanoparticles in the environment: where do we come from, where do we go to? Env. Sci. Eur. 30 (1), 6. https://doi.org/10.1186/s12302-018-0132-6.

Cerrillo, C., Barandika, G., Igartua, A., Areitioaurtena, O., Mendoza, G., 2016. Towards the standardization of nanoecotoxicity testing: natural organic matter 'camouflages' the adverse effects of TiO_2 and CeO_2 nanoparticles on green microalgae. Sci. Total Env. 543 (Pt A), 95–104. https://doi.org/10.1016/j.scitotenv.2015.10.137.

Cheloni, G., Cosio, C., Slaveykova, V.I., 2014. Antagonistic and synergistic effects of light irradiation on the effects of copper on *Chlamydomonas reinhardtii*. Aquat. Toxicol. 155, 275–282. https://doi.org/10.1016/j.aquatox.2014.07.010.

Connor, P.A., McQuillan, A.J., 1999. Phosphate adsorption onto TiO_2 from aqueous solutions: an in situ internal reflection infrared spectroscopic study. Langmuir. 15 (8), 2916–2921. https://doi.org/10.1021/la980894p.

Dar, G.I., Saeed, M., Wu, A., 2020. Toxicity of TiO_2-NPs. In: Wu, A., Ren, W. (Eds.), TiO_2 Nanoparticles: Applications in Nanobiotechnology and Nanomedicine. Wiley-VCH Verlag GmbH & Co. KGaA. https://doi.org/10.1002/9783527825431.

Dedman, C.J., Rizk, M.M.I., Christie-Oleza, J.A., Davies, G.L., 2021. Investigating the impact of cerium oxide nanoparticles upon the ecologically significant marine cyanobacterium *Prochlorococcus*. Front. Mar. Sci. 8. https://doi.org/10.3389/fmars.2021.668097.

Deng, X.Y., Cheng, J., Hu, X.L., Wang, L., Li, D., Gao, K., 2017. Biological effects of TiO_2 and CeO_2 nanoparticles on the growth, photosynthetic activity, and cellular components of a marine diatom *Phaeodactylum tricornutum*. Sci Total Env. 575, 87–96. https://doi.org/10.1016/j.scitotenv.2016.10.003.

Deng, Z., Lin, Z., Zou, X., Yao, Z., Tian, D., Wang, D., Yin, D., 2012. Model of hormesis and its toxicity mechanism based on quorum sensing: a case study on the toxicity of sulfonamides to *Photobacterium phosphoreum*. Env. Sci. Technol. 46 (14), 7746–7754. https://doi.org/10.1021/es203490f.

Dobesova, M., Kolackova, M., Pencik, O., Capal, P., Chaloupsky, P., Svec, P., Ridoskova, A., Motola, M., Cicmancova, V., Sopha, H., Macak, J.M., Richtera, L., Adam, V., Huska, D., 2023. Transcriptomic hallmarks of in vitro TiO_2 nanotubes toxicity in *Chlamydomonas reinhardtii*. Aquat. Toxicol. 256, 106419. https://doi.org/10.1016/j.aquatox.2023.106419.

Domingos, R.F., Peyrot, C., Wilkinson, K.J., 2010. Aggregation of titanium dioxide nanoparticles: role of calcium and phosphate. Env. Chem. 7 (1), 61–66. https://doi.org/10.1071/en09110.

Geitner, N.K., Marinakos, S.M., Guo, C., O'Brien, N., Wiesner, M.R., 2016. Nanoparticle surface affinity as a predictor of trophic transfer. Env. Sci. Technol 50 (13), 6663–6669. https://doi.org/10.1021/acs.est.6b00056.

Ghazaei, F., Shariati, M., 2020. Effects of titanium nanoparticles on the photosynthesis, respiration, and physiological parameters in *Dunaliella salina* and *Dunaliella tertiolecta*. Protoplasma 257 (1), 75–88. https://doi.org/10.1007/s00709-019-01420-z.

Haddad, M., Frickenstein, A.N., Wilhelm, S., 2023. High-throughput single-cell analysis of nanoparticle-cell interactions. TrAC Trends Anal. Chem. 166, 117172. https://doi.org/10.1016/j.trac.2023.117172.

Hamed, S.M., El Tablawy, N.H., Mohamed, M.Y.A., Alammari, B.S., AbdElgawad, H., 2024. Accumulation and nano-ecotoxicological impact of cerium oxide nanoparticles on cyanobacteria: understanding photosynthesis, detoxification, and antioxidant responses. J. Env. Chem. Eng. 12 (2). https://doi.org/10.1016/j.jece.2024.112134.

Hu, J., Wu, D., Lin, X., Cheng, W., 2025. Facet-dependent phosphate adsorption of CeO_2. Ind. Eng. Chem. Res. 64 (3), 1544–1554. https://doi.org/10.1021/acs.iecr.4c02763.

Huang, Y., Gao, M., Wang, W., Liu, Z., Qian, W., Chen, C.C., Zhu, X., Cai, Z., 2022. Effects of manufactured nanomaterials on algae: implications and applications. Front. Environ. Sci. Eng. 16 (9), 122. https://doi.org/10.1007/s11783-022-1554-3.

Hund-Rinke, K., Schlich, K., Kühnel, D., Hellack, B., Kaminski, H., Nickel, C., 2018. Grouping concept for metal and metal oxide nanomaterials with regard to their ecotoxicological effects on algae, daphnids and fish embryos. NanoImpact. 9, 52–60. https://doi.org/10.1016/j.impact.2017.10.003.

Hund-Rinke, K., Sinram, T., Schlich, K., Nickel, C., Dickehut, H.P., Schmidt, M., Kuhnel, D., 2020. Attachment efficiency of nanomaterials to algae as an important criterion for ecotoxicity and grouping. Nanomaterials. (Basel) (6), 10. https://doi.org/10.3390/nano10061021.

Joonas, E., Aruoja, V., Olli, K., Kahru, A., 2019. Environmental safety data on CuO and TiO_2 nanoparticles for multiple algal species in natural water: filling the data gaps for risk assessment. Sci. Total Env. 647, 973–980. https://doi.org/10.1016/j.scitotenv.2018.07.446.

Kahru, A., Ivask, A., 2013. Mapping the ddawn of nanoecotoxicological research. Acc. Chem. Res. 46 (3), 823–833. https://doi.org/10.1021/ar3000212.

Kosak Nee Rohder, L.A., Brandt, T., Sigg, L., Behra, R., 2018. Uptake and effects of cerium(III) and cerium oxide nanoparticles to *Chlamydomonas reinhardtii*. Aquat. Toxicol. 197, 41–46. https://doi.org/10.1016/j.aquatox.2018.02.004.

Lead, J.R., Batley, G.E., Alvarez, P.J.J., Croteau, M.N., Handy, R.D., McLaughlin, M.J., Judy, J.D., Schirmer, K., 2018. Nanomaterials in the environment: behavior, fate, bioavailability, and effects - An updated review. Environ. Toxicol. Chem. 37 (8), 2029–2063. https://doi.org/10.1002/etc.4147.

Lee, S.H., Jung, K., Chung, J., Lee, Y.W., 2022. Comparative study of algae-based measurements of the toxicity of 14 manufactured nanomaterials. Int. J. Env. Res Public Health 19 (10). https://doi.org/10.3390/ijerph19105853.

Li, F., Liang, Z., Zheng, X., Zhao, W., Wu, M., Wang, Z., 2015. Toxicity of nano-TiO_2 on algae and the site of reactive oxygen species production. Aquat. Toxicol. 158, 1–13. https://doi.org/10.1016/j.aquatox.2014.10.014.

Liu, S., Han, J., Ma, X., Zhu, X., Qu, H., Xin, G., Huang, X., 2024. Repeated release of cerium oxide nanoparticles altered algal responses: growth, photosynthesis, and photosynthetic gene expression. Eco Env. Health 3 (3), 290–299. https://doi.org/10.1016/j.eehl.2024.04.002.

Liu, W., Li, M., Li, W., Keller, A.A., Slaveykova, V.I., 2022. Metabolic alterations in alga *Chlamydomonas reinhardtii* exposed to $nTiO_2$ materials. Env. Sci Nano 9 (8), 2922–2938. https://doi.org/10.1039/d2en00260d.

Liu, W., Worms, I.A., Slaveykova., V.I., 2021. Interactions of metal-containing nanomaterials with microorganisms, in: Gupta, M.N., Khare, S.K., & Sinha, R. (Eds.) (Ed.) Interfaces Between Nanomaterials and Microbes. RC Press, pp. 38–57. https://doi.org/10.1201/9780429321269.

Lum, J.T., Leung, K.S., 2019. Quantifying silver nanoparticle association and elemental content in single cells using dual mass mode in quadrupole-based inductively coupled plasma-mass spectrometry. Anal. Chim. Acta 1061, 50–59. https://doi.org/10.1016/j.aca.2019.02.042.

Mackevica, A., Hendriks, L., Meili-Borovinskaya, O., Baun, A., Skjolding, L.M., 2023. Effect of exposure concentration and growth conditions on the association of cerium oxide nanoparticles with green algae. Nanomaterials (Basel) (17), 13. https://doi.org/10.3390/nano13172468.

Mahana, A., Guliy, O.I., Mehta, S.K., 2021. Accumulation and cellular toxicity of engineered metallic nanoparticle in freshwater microalgae: current status and future challenges. Ecotoxicol. Env. Saf. 208, 111662. https://doi.org/10.1016/j.ecoenv.2020.111662.

Mahaye, N., Musee, N., 2023. Evaluation of apical and molecular effects of algae *Pseudokirchneriella subcapitata* to cerium oxide nanoparticles. Toxics. 11 (3). https://doi.org/10.3390/toxics11030283.

Manier, N., Bado-Nilles, A., Delalain, P., Aguerre-Chariol, O., Pandard, P., 2013. Ecotoxicity of non-aged and aged CeO_2 nanomaterials towards freshwater microalgae. Env. Pollut. 180, 63–70. https://doi.org/10.1016/j.envpol.2013.04.040.

Merrifield, R.C., Stephan, C., Lead, J.R., 2018. Quantification of Au nanoparticle biouptake and distribution to freshwater algae using single cell - ICP-MS. Env. Sci. Technol. 52 (4), 2271–2277. https://doi.org/10.1021/acs.est.7b04968.

Middepogu, A., Hou, J., Gao, X., Lin, D., 2018. Effect and mechanism of TiO_2 nanoparticles on the photosynthesis of *Chlorella pyrenoidosa*. Ecotoxicol. Env. Saf. 161, 497–506. https://doi.org/10.1016/j.ecoenv.2018.06.027.

Mohajeri, M., Momenai, R., Karami-Mohajeri, S., Ohadi, M., Raeisi Estabragh, M.A., 2025. Cerium oxide nanoparticles, physical and chemical properties, applications and toxicological implications: a review. Results. Chem. 15, 102302. https://doi.org/10.1016/j.rechem.2025.102302.

Musial, J., Krakowiak, R., Mlynarczyk, D.T., Goslinski, T., Stanisz, B.J., 2020. Titanium dioxide nanoparticles in food and personal care products-what do we know about their safety? Nanomaterials (Basel) (6), 10. https://doi.org/10.3390/nano10061110.

Nguyen, M.K., Moon, J.Y., Lee, Y.C., 2020. Microalgal ecotoxicity of nanoparticles: an updated review. Ecotoxicol. Env. Saf. 201, 110781. https://doi.org/10.1016/j.ecoenv.2020.110781.

Nogueira, V., Lopes, I., Rocha-Santos, T.A., Rasteiro, M.G., Abrantes, N., Goncalves, F., Soares, A.M., Duarte, A.C., Pereira, R., 2015. Assessing the ecotoxicity of metal nano-oxides with potential for wastewater treatment. Env. Sci. Pollut. R 22 (17), 13212–13224. https://doi.org/10.1007/s11356-015-4581-9.

OECD, 2011. Test No. 201: Freshwater Alga and Cyanobacteria, Growth Inhibition Test. OECD Publishing, Paris, OECD Guidelines for the Testing of Chemicals, Section 2: Effects on Biotic Systems. OECD Publishing, New York, NY, USA.

Ozkaleli, M., Erdem, A., 2018. Biotoxicity of TiO_2 nanoparticles on *Raphidocelis subcapitata* microalgae exemplified by membrane deformation. Int. J. Env. Res Public Health 15 (3). https://doi.org/10.3390/ijerph15030416.

Pace, H.E., Rogers, N.J., Jarolimek, C., Coleman, V.A., Higgins, C.P., Ranville, J.F., 2011. Determining transport efficiency for the purpose of counting and sizing nanoparticles via single particle inductively coupled plasma mass spectrometry. Anal. Chem. 83 (24), 9361–9369. https://doi.org/10.1021/ac201952t.

Pansambal, S., Oza, R., Borgave, S., Chauhan, A., Bardapurkar, P., Vyas, S., Ghotekar, S., 2022. Bioengineered cerium oxide CeO_2 nanoparticles and their diverse applications: a review. Appl. Nanosci. 13 (9), 6067–6092. https://doi.org/10.1007/s13204-022-02574-8.

Pulido-Reyes, G., Briffa, S.M., Hurtado-Gallego, J., Yudina, T., Leganés, F., Puntes, V., Valsami-Jones, E., Rosal, R., Fernández-Piñas, F., 2019. Internalization and toxicological mechanisms of uncoated and PVP-coated cerium oxide nanoparticles in the freshwater alga *Chlamydomonas reinhardtii*. Environ. Sci. 6 (6), 1959–1972. https://doi.org/10.1039/c9en00363k.

Rasmussen, K., Jan Mast, P.J.D.T., Eveline Verleysen, N.W., Steen, F.V., Pizzolon, J.C., Temmerman, L.D., Doren, E.V., Jensen, K.A., Birkedal, R., Levin, M., Nielsen, S.H., Koponen, I.K., Clausen, P.A., Kofoed-Sørensen, V., Kembouche, Y., Thieriet, N., Spalla, O., Guiot, C., Rousset, D., Witschger, O., Bau, S., Bianchi, B., Motzkus, C., Shivachev, B., Dimowa, L., Nikolova, R., Nihtianova, D., Tarassov, M., Petrov, O., Bakardjieva, S., Gilliland, D., Pianella, F., Ceccone, G., Spampinato, V., Cotogno, G., Gibson, N., Gaillard, C., Mech, A., 2014. Titanium Dioxide, NM-100, NM-101, NM-102, NM-103, NM-104, NM-105: Characterisation and Physico-Chemical Properties. https://doi.org/10.2788/79554.

Rivero Arze, A., Manier, N., Chatel, A., Mouneyrac, C., 2020. Characterization of the nano-bio interaction between metallic oxide nanomaterials and freshwater microalgae using flow cytometry. Nanotoxicology 14 (8), 1082–1095. https://doi.org/10.1080/17435390.2020.1808106.

Rodea-Palomares, I., Boltes, K., Fernandez-Pinas, F., Leganes, F., Garcia-Calvo, E., Santiago, J., Rosal, R., 2011. Physicochemical characterization and ecotoxicological assessment of CeO_2 nanoparticles using two aquatic microorganisms. Toxicol. Sci. 119 (1), 135–145. https://doi.org/10.1093/toxsci/kfq311.

Sanchez-Garcia, L., Bolea, E., Laborda, F., Cubel, C., Ferrer, P., Gianolio, D., da Silva, I., Castillo, J.R., 2016. Size determination and quantification of engineered cerium oxide nanoparticles by flow field-flow fractionation coupled to inductively coupled plasma mass spectrometry. J. Chromatogr. A 1438, 205–215. https://doi.org/10.1016/j.chroma.2016.02.036.

Sendra, M., Yeste, P.M., Moreno-Garrido, I., Gatica, J.M., Blasco, J., 2017. CeO_2 NPs, toxic or protective to phytoplankton? Charge of nanoparticles and cell wall as factors which cause changes in cell complexity. Sci. Total Environ. 590-591 304–315. https://doi.org/10.1016/j.scitotenv.2017.03.007.

Siciliano, A., Spampinato, M., Salbitani, G., Guida, M., Carfagna, S., Brouziotis, A.A., Trifuoggi, M., Bossa, R., Saviano, L., Padilla Suarez, E.G., Libralato, G., 2024. Multi-endpoint analysis of cerium and gadolinium effects after long-term exposure to *Phaeodactylum tricornutum*. Environments 11 (3). https://doi.org/10.3390/environments11030058.

Singh, C., Steffi, F., Ceccone, G., Gibson, N., Jensen, A., Levin, M., Goenaga-Infante, H., David, C., Rasmussen, K., 2014. Cerium dioxide, NM-211, NM-212, NM-213. Characterisation and test item preparation. JRC Sci. Policy Rep. https://doi.org/10.2788/80203.

Sivakumar, M., Dhinakarasamy, I., Chakraborty, S., Clements, C., Thirumurugan, N.K., Chandrasekar, A., Vinayagam, J., Kumar, C., Thirugnanasambandam, R., Kumar, V. R., Chandrasekaran, V.N., 2025. Effects of titanium oxide nanoparticles on growth, biochemical composition, and photosystem mechanism of marine microalgae *Isochrysis galbana* COR-A3. Nanotoxicology 19 (2), 156–179. https://doi.org/10.1080/17435390.2025.2454267.

Skjolding, L.M., Sorensen, S.N., Dyhr, K.S., Hjorth, R., Schluter, L., Hedberg, C., Hartmann, N.B., Mayer, P., Baun, A., 2022. Separating toxicity and shading in algal growth inhibition tests of nanomaterials and colored substances. Nanotoxicology 16 (3), 265–275. https://doi.org/10.1080/17435390.2022.2080608.

Slaveykova, V.I., Li, M., Worms, I.A., Liu, W., 2020. When environmental chemistry meets ecotoxicology: bioavailability of inorganic nanoparticles to phytoplankton. CHIMIA 74 (3), 115. https://doi.org/10.2533/chimia.2020.115.

Suárez-Oubiña, C., Herbello-Hermelo, P., Bermejo-Barrera, P., Moreda-Piñeiro, A., 2022. Exploiting dynamic reaction cell technology for removal of spectral interferences in the assessment of Ag, Cu, Ti, and Zn by inductively coupled plasma mass spectrometry. Spectrochim. Acta. B 187. https://doi.org/10.1016/j.sab.2021.106330.

Taylor, N.S., Merrifield, R., Williams, T.D., Chipman, J.K., Lead, J.R., Viant, M.R., 2016. Molecular toxicity of cerium oxide nanoparticles to the freshwater alga *Chlamydomonas reinhardtii* is associated with supra-environmental exposure concentrations. Nanotoxicology 10 (1), 32–41. https://doi.org/10.3109/17435390.2014.1002868.

Thiagarajan, V., Alex, S.A., Seenivasan, R., Chandrasekaran, N., Mukherjee, A., 2021. Toxicity evaluation of nano-TiO_2 in the presence of functionalized microplastics at two trophic levels: algae and crustaceans. Sci. Total Env. 784, 147262. https://doi.org/10.1016/j.scitotenv.2021.147262.

Thiagarajan, V., Ramasubbu, S., 2022. Extraction and characterization of sub-micron sized TiO_2 from toothpaste: evaluation of their toxic effects in marine microalgae *Chlorella* sp. Toxicol. Env. Health 14 (2), 147–155. https://doi.org/10.1007/s13530-022-00124-x.

Thiagarajan, V., Ramasubbu, S., Natarajan, C., Mukherjee, A., 2019. Differential sensitivity of marine algae *Dunaliella salina* and *Chlorella* sp. to P25 TiO_2 NPs. Env. Sci. Pollut. R 26 (21), 21394–21403. https://doi.org/10.1007/s11356-019-05332-6.

Vijver, M.G., Zhai, Y., Wang, Z., Peijnenburg, W.J.G.M., 2018. Emerging investigator series: the dynamics of particle size distributions need to be accounted for in bioavailability modelling of nanoparticles. Environ. Sci. 5 (11), 2473–2481. https://doi.org/10.1039/C8EN00572A.

von Moos, N., Bowen, P., Slaveykova, V.I., 2014. Bioavailability of inorganic nanoparticles to planktonic bacteria and aquatic microalgae in freshwater. Environ. Sci. 1 (3), 214–232. https://doi.org/10.1039/C3EN00054K.

von Moos, N., Maillard, L., Slaveykova, V.I., 2015. Dynamics of sub-lethal effects of nano-CuO on the microalga *Chlamydomonas reinhardtii* during short-term exposure. Aquat. Toxicol. 161, 267–275. https://doi.org/10.1016/j.aquatox.2015.02.010.

von Moos, N., Slaveykova, V.I., 2014. Oxidative stress induced by inorganic nanoparticles in bacteria and aquatic microalgae –state of the art and knowledge gaps. Nanotoxicology 8 (6), 605–630. https://doi.org/10.3109/17435390.2013.809810.

Wang, D., Mao, W., Zhao, L., Meng, D., Wu, T., 2024. Effects of aggregation and settling of photoactive TiO_2 nanoparticles on *Microcystis aeruginosa* and extracellular matters release. Algal. Res. 82. https://doi.org/10.1016/j.algal.2024.103626.

Wang, Y., Zhu, X., Lao, Y., Lv, X., Tao, Y., Huang, B., Wang, J., Zhou, J., Cai, Z., 2016. TiO_2 nanoparticles in the marine environment: physical effects responsible for the toxicity on algae *Phaeodactylum tricornutum*. Sci. Total. Env. 565, 818–826. https://doi.org/10.1016/j.scitotenv.2016.03.164.

Wu, D., Yang, S., Du, W., Yin, Y., Zhang, J., Guo, H., 2019. Effects of titanium dioxide nanoparticles on *Microcystis aeruginosa* and microcystins production and release. J. Hazard. Mater. 377, 1–7. https://doi.org/10.1016/j.jhazmat.2019.05.013.

Wu, D., Zhang, J., Du, W., Yin, Y., Guo, H., 2022. Toxicity mechanism of cerium oxide nanoparticles on cyanobacteria *Microcystis aeruginosa* and their ecological risks. Env. Sci. Pollut. R 29 (23), 34010–34018. https://doi.org/10.1007/s11356-021-18090-1.

Xia, B., Chen, B., Sun, X., Qu, K., Ma, F., Du, M., 2015. Interaction of TiO_2 nanoparticles with the marine microalga *Nitzschia closterium*: growth inhibition, oxidative stress and internalization. Sci. Total Env. 508, 525–533. https://doi.org/10.1016/j.scitotenv.2014.11.066.

Xie, C., Ma, Y., Zhang, P., Zhang, J., Li, X., Zheng, K., Li, A., Wu, W., Pang, Q., He, X., Zhang, Z., 2021. Elucidating the origin of the toxicity of nano-CeO_2 to *Chlorella pyrenoidosa:* the role of specific surface area and chemical composition. Environ. Sci. 8 (6), 1701–1712. https://doi.org/10.1039/d0en01177k.

Xu, F., 2018. Review of analytical studies on TiO_2 nanoparticles and particle aggregation, coagulation, flocculation, sedimentation, stabilization. Chemosphere 212, 662–677. https://doi.org/10.1016/j.chemosphere.2018.08.108.

Yu, F.P., Gao, J.T., Zhang, P., Tang, S.K., Liu, H.J., Li, W.P., 2025. Distribution, environmental behavior, and ecotoxicity of different metal oxide nanoparticles in the aquatic environment. Process. Saf. Environ. Prot. 196. https://doi.org/10.1016/j.psep.2025.106856.

Zeng, H., Lv, Z., Sun, X., Tong, Y., Wu, W., Dong, S., Mao, L., 2024a. Predicting bioaccumulation of nanomaterials: modeling approaches with challenges. Env. Health (Wash) 2 (4), 189–201. https://doi.org/10.1021/envhealth.3c00138.

Zeng, Y.L., Molnárová, M., Motola, M., 2024b. Metallic nanoparticles and photosynthesis organisms: comprehensive review from the ecological perspective. J. Env. Manage 358. https://doi.org/10.1016/j.jenvman.2024.120858.

Zheng, Y., Nowack, B., 2022. Meta-analysis of bioaccumulation data for nondissolvable engineered nanomaterials in freshwater aquatic organisms. Environ. Toxicol. Chem. 41 (5), 1202–1214. https://doi.org/10.1002/etc.5312.

Zhu, L., Booth, A.M., Feng, S., Shang, C., Xiao, H., Tang, X., Sun, X., Zhao, X., Chen, B., Qu, K., Xia, B., 2022. UV-B radiation enhances the toxicity of TiO_2 nanoparticles to the marine microalga *Chlorella pyrenoidosa* by disrupting the protection function of extracellular polymeric substances. Environ. Sci. 9 (5), 1591–1604. https://doi.org/10.1039/d1en01198g.

Zucker, R.M., Massaro, E.J., Sanders, K.M., Degn, L.L., Boyes, W.K., 2010. Detection of TiO_2 nanoparticles in cells by flow cytometry. Cytom. A 77A (7), 677–685. https://doi.org/10.1002/cyto.a.20927.